ISSN 1063-4576, Journal of Superhard Materials, 2016, Vol. 38, No. 2, pp. 114–122. © Allerton Press, Inc., 2016.
Original Russian Text © V.M. Beresnev, S.A. Klimenko, O.V. Sobol', S.S. Grankin, V.A. Stolbovoi, P.V. Turbin, V.Yu. Novikov, A.A. Meilekhov, S.V. Litovchenko, L.V. Malikova, 2016, published in Sverkhtverdye Materialy, 2016, Vol. 38, No. 2, pp. 55–64.

Effect of the Deposition Parameters on the Phase–Structure State, Hardness, and Tribological Characteristics of Mo_2N/CrN Vacuum–Arc Multilayer Coatings

V. M. Beresnev[a, *], S. A. Klimenko[b], O.V. Sobol'[c], S. S. Grankin[a], V. A. Stolbovoi[d], P. V. Turbin[a, e], V. Yu. Novikov[f], A. A. Meilekhov[c], S. V. Litovchenko[a], and L. V. Malikova[e]

[a] *Karazin Khar'kiv National University, pl. Svobody 4, Khar'kiv, 61022 Ukraine*

[b] *Bakul Institute for Superhard Materials, National Academy of Sciences of Ukraine, vul. Avtozavods'ka 2, Kiev, 04074 Ukraine*

[c] *Khar'kovskii Polytechnic Institute National Technical University, ul. Frunze 21, Khar'kiv, 61002 Ukraine*

[d] *National Scientific Center Kharkiv Institute of Physics and Technology, vul. Akademichna, 1, Khar'kiv, 61108 Ukraine*

[e] *Scientific Physico-Technological Center of the Ministry of Education and National Academy of Sciences of Ukraine, pl. Svobody 6, Khar'kiv, 61022 Ukraine*

[f] *Belgorod State University, ul. Pobedy 85, Belgorod, 308015 RF*

**e-mail: beresnev-sept@yandex.ru*

Received September 2, 2015

Abstract—A complex study has been performed of the effect of the technological parameters, which are responsible for the energy states of deposited particles, on the elemental, phase and structure compositions, hardness, and tribological characteristics of formed vacuum–arc multilayer Mo_2N/CrN systems with a nanometric thickness. The formation of two phase and structure types has been defined in combined nitride layers: γ-Mo_2N/CrN with the isostructural cubic crystalline lattices and γ-Mo_2N/CrN with non-isostructural cubic and hexagonal lattices.

DOI: 10.3103/S1063457616020052

Keywords: vacuum–arc deposition, multilayer coatings, tribological characteristics.

1. INTRODUCTION

Nitrides of transition metals are characterized by the high melting temperature (2300–3400°C), high hardness, and high electrical conductivity characteristic of metals. The main disadvantage is a high brittleness, whose value may be essentially decreased by the formation of the nanostructural status of the material [1–5].

One of the most promising lines of improving operational characteristics of nitride coatings is a development of multilayer structures with a nanometric thickness of layers. By alternating two or more material layers having different physico-mechanical characteristics it is possible to largely change the system properties including the stress-strained state and prerequisites to crack propagation, as a result of which the fracture toughness of such a composite increases.

Structural state and properties of the MoN and CrN layers of multilayer coatings may vary over a wide range depending on the voltage supplied onto a substrate and a pressure of nitrogen atmosphere during the deposition [6–9]. In this connection one may expect a considerable sensitivity to the physicotechnical parameters of the deposition of structural states and properties of coatings based on MoN and CrN as layers of a multilayer system. The highest effects may be expected in the case that the layers are of nanometric thicknesses, which stems from the fact that nitrides exhibit the highest mechanical properties in this dimensional range [10–12].

2. EXPERIMENTAL

Samples were prepared by the vacuum–arc method on a modernized Bulat-6 plant [13]. Pressure of nitrogen in the course of the deposition was $p_N = (7–30) \times 10^{-4}$ Torr, the deposition rate was about 3 nm/s.

Coatings were deposited using two targets (Mo and Cr) at the continuous rotation of samples fixed on substrates. The rotation rate was 8 rev/min, which made it possible to deposit a coating about 9 mm thick (with separate layers 10 nm in thickness) for 1h. A total amount of layers was 960 or 480 bilayer periods. During the deposition a constant negative bias voltage was supplied onto substrates at the values of $U_b = 20$, 70, 150, and 300 V.

Phase and structure were analyzed by X-ray diffraction in the CuKα radiation. The profiles were divided into components using the NewProfile software package.

The hardness was measured by microindentation on a 402MVD device of the Instron Wolpert Wilson Instruments company using a Vickers diamond pyramid at loadings of 25, 50, and 100 g.

The adhesion and cohesion strengths, resistance against scratching, and detection of the coating fracture mechanism were defined using a Revetest ("CSM Instruments") scratch–tester. The scratches were made on the coating surface by a diamond spherical indenter of the Rockwell C type with the tip radius of 200 μm during the continuously increasing loading from 0 to 200 N at the resolution not worse than 3 mN. At the same time we registered the power of acoustic emission signal, friction coefficient, depth of the indenter penetration, and the normal indentation load. To obtain reliable results, we made three scratches on the surface of each sample. The tests were conducted at the following conditions: the indentation load varied from 0.9 to 70 N, rate of the indenter displacement was 1 mm/min, scratch length was 10 mm, rate of load application was 6.91 N/min, frequency of the signal discreteness was 60 Hz, AE signal power was 9 dB. In the course of testing we defined the minimum (critical) loads: L_{c1} that corresponds to the beginning of the indenter penetration into the coating, L_{c2} that corresponds to appearance of cracks accumulation, and L_{c3} corresponds to the spalling of the coating or to its plastic abrasion to the substrate.

Tribological tests were carried out in air by the ball-on-disk scheme on a Tribometer friction machine (CSM Instruments). The samples were discs of steel 45 (55 HRC), onto polished surface of which coatings with the surface roughness *Ra* 0.08 μm were deposited. As counterbodies we used balls 6.0 mm in diameter manufactured of sintered certified aluminum oxide Al_2O_3.

In accordance with the ASTM G99·959, DIN 50324, and ISO 20808 international standards, the testing load was 3.0 N and sliding velocity 10 cm/s.

The morphology of wear grooves on the coating and wear spots on balls were studied with the use of an Olympus GX 51 optical inverted microscope and a FEI Nova NanoSEM 450 scanning electron microscope. The wear resistances of the samples and counterbodies were assessed from the wear factor, *W*, the calculation procedure of which is given in [14].

3. RESULTS AND DISCUSSION

The energy dispersive analysis of coatings showed that bias voltage exerted a decisive effect on the variation of the nitrogen contents of coatings produced at lower pressure ($p_N = 7 \times 10^{-4}$ Torr) (Fig. 1, curve *1*). Evidently, the reason for this is a secondary selective sputtering of light atoms of nitrogen from a formed surface of the coating. In this case, a relatively high energy of film-forming hard metal atoms of Mo and Cr exerts a decisive effect (energy losses by collision at low pressure during the deposition are minimized).

At a higher pressure ($p_N = 10^{-3}$ Torr) with increasing the negative bias voltage up to 150 V a small increase of the nitrogen content of coatings is observed, which defines an improvement of the efficiency of the nitride formation [4] and only at $U_b = 300$ V the nitrogen concentration decreases, which is caused by a selective secondary sputtering.

A phase and structure analysis of the coatings states based on the X-ray diffraction spectra (Fig. 2) shows that as the bias voltage increases at a small pressure of ($p_N = 3 \times 10^{-3}$ Torr), a coordinated transition from the preferred orientation with the [111] axis to the preferred orientation with the [100] axis takes place, which shows up in a relative change of the intensities of (111) and (200) reflexes, respectively,.

In this case we observe the agreement of the structures of nitrogen nanolayers (111)γ-Mo_2N/(111)CrN and (200)γ-Mo_2N/(200)CrN with cubic (structural type NaCl, cards JCPDS 11-0065 and JCPDS 25-1366, respectively) crystal lattices. However, at the bias voltage, highest by the modulus (U_b= 300 V), in chromium

nitride (CrN) layers the β-Cr_2N phase with the hexagonal crystal lattice (card JCPDS 35-0803) appears because of a decrease of the nitrogen concentration. The appearance of the lower by nitrogen β-Cr_2N phase at a lower ($p_N = 7 \times 10^{-4}$ Torr) pressure is even more clearly expressed (see Fig. 2, spectrum *3*), and a texture with the [001] axis forms in chromium nitride layers.

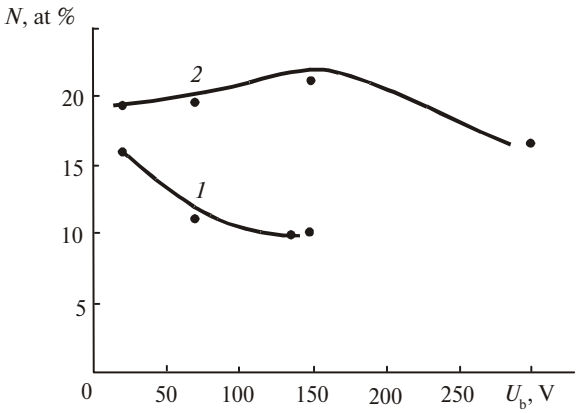

Fig. 1. Variations of the nitrogen, N, concentration in a coating depending on bias voltage, U_b, at pressures of $p_N = 7 \times 10^{-4}$ (*1*) and 3×10^{-3} (*2*) Torr.

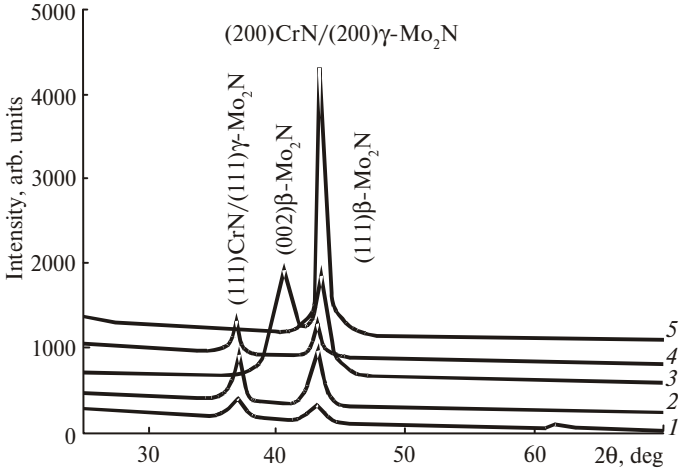

Fig. 2. Sections of diffraction spectra of coatings produced at $p_N = 3 \times 10^{-3}$ (*1*, *2*, *4*, *5*) and 7×10^{-4} (*3*) Torr; negative bias voltage $U_b =$ 20 (*1*), 70 (*2*, *3*), 150 (*4*), 300 (*5*) V.

A wide spectrum of coatings structural states defines considerable changes in its mechanical characteristics. Thus, from the dependence of the hardness, *H*, on the bias voltage, U_b, given in Fig. 3 it is seen that the highest hardness is attained at the lowest (by modulus) bias voltage, U_b, and high nitrogen pressure, p_N, which provides the highest nitrogen concentration. A decrease in hardness at the lower pressure may be attributed to the formation of vacancies in the sublattice of nitrogen, due to its much lower content of coating as compared with the stoichiometric composition of CrN chromium and Mo_2N molybdenum nitrides.

The reason for a decrease in hardness as the modulus of the bias voltage increases is the intensification of the mixing in a near-boundary region, which in relatively thin (about 10 nm) layers of a coating leads to a large share of the mixed region with a state of a solid solution and decreased hardness because of it.

The values of the friction coefficient, μ, wear intensity, *v*, and the parameter of the surface roughness, *Ra*, obtained by tribological testing of the Mo_2N/CrN coatings at various working pressures of nitrogen are given in Table 1.

Our studies of the friction characteristics in dry friction of coatings with the counterbody of Al_2O_3 (see Table 1) show considerable differences of the wear intensities of coatings formed at different nitrogen pressures. Coatings produced at the high ($p_N = 3 \times 10^{-3}$ Torr) pressure are characterized by single-phase layer

having the same type of the cubic crystalline lattice (see Fig. 3). Coatings deposited at low ($p_N = 7 \times 10^{-4}$ Torr) pressure are formed by layers of chromium nitride, CrN, with a phase having a hexagonal crystal lattice (see Fig. 3). This phase is the lowest by nitrogen. In this case there form different types of crystal lattices with a high discrepancy of interphase boundaries of contact in layers.

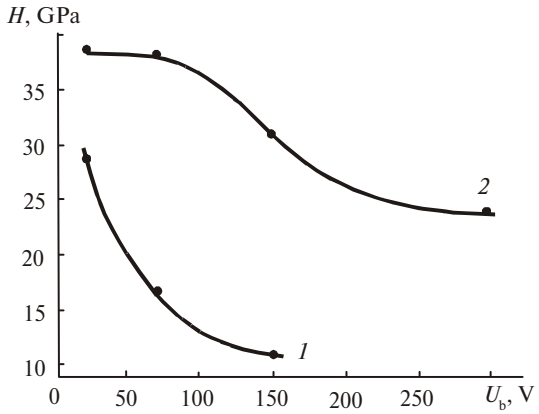

Fig. 3. Dependence of coatings hardness on the applied negative bias voltage U_b at $p_N = 7 \times 10^{-4}$ (*1*), 3×10^{-3} (*2*) Torr.

Table 1. Tribological characteristics of Mo_2N/CrN coatings produced at the negative bias voltage $U_b = 70$ V and various pressures of nitrogen

Pressure	Friction coefficient, μ		Wear intensity, ν, $mm^3 \cdot H^{-1} \cdot m^{-1}$		*Ra*, μm
	initial	during the tests	counterbody (Al_2O_3)	coating	
7×10^{-4} Torr	0.381	0.586	0.25×10^{-7}	13.45×10^{-7}	0.47
3×10^{-3} Torr	0.535	0.579	0.86×10^{-7}	6.36×10^{-7}	0.28

Thus, it follows from Table 1 that at low pressure, when in MoN and CrN layers the formation of phases that differ in crystal lattice takes place, the coating has an increased brittleness and wears more intensively than the counterbody. As the pressure increases and conjugation of cubic lattices appears in the coating layers (at high pressure $p_N = 3 \times 10^{-3}$ Torr), its wear resistance increases.

Figures 4 and 5 show the initial surfaces of coating, contact regions of the counterbody, wear tracks on the coating and their transverse profiles.

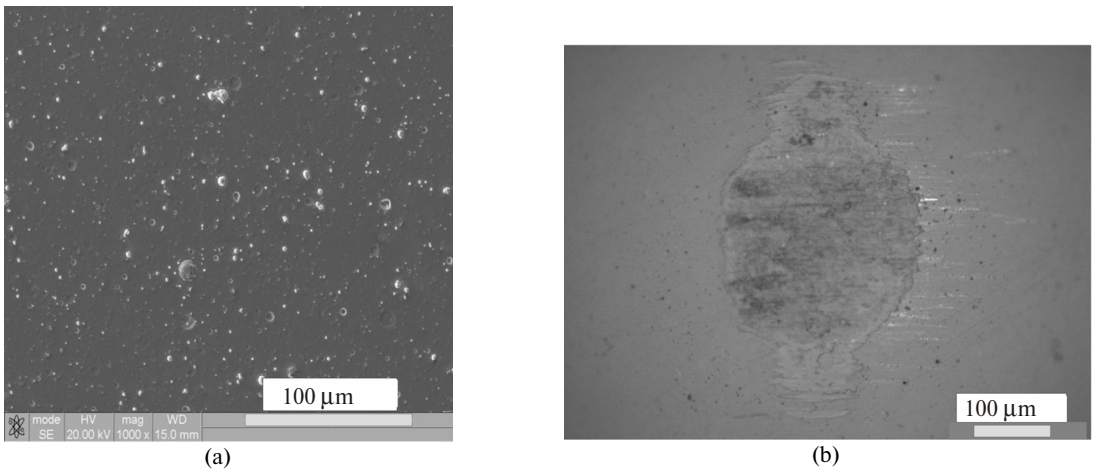

(a) (b)

Fig. 4. Initial surface of the Mo_2N/CrN coating, produced at $p_N = 7 \times 10^{-4}$ Torr (a), contact region of the counterbody (b), wear track on the coating (c) and its transverse profile (d).

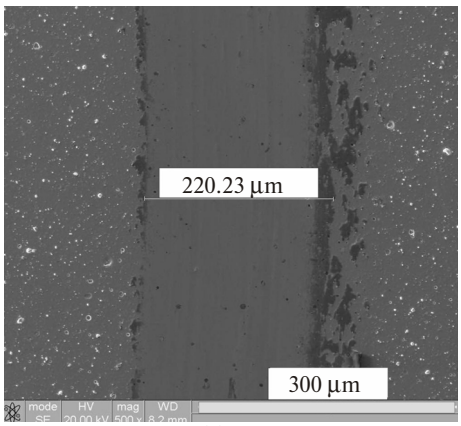

(c)

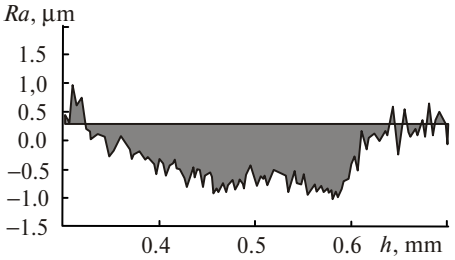

(d)

Fig. 4. (Contd.)

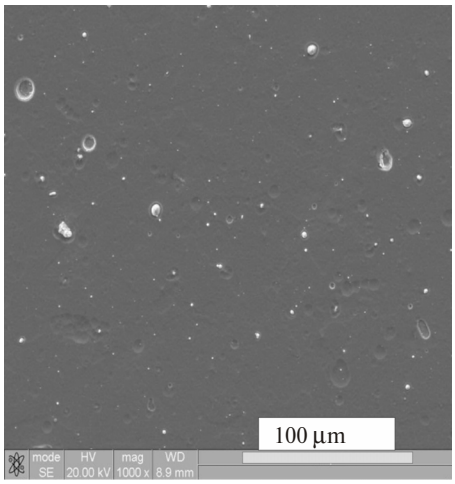

(a)

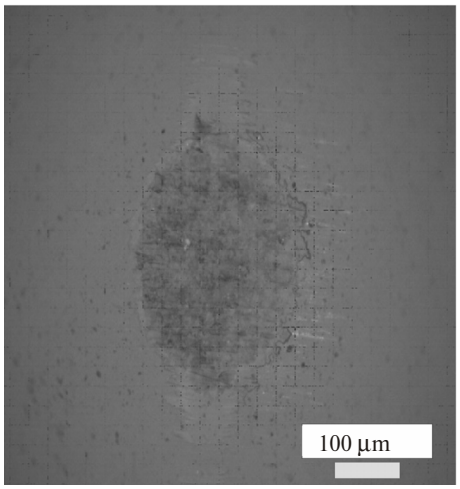

(b)

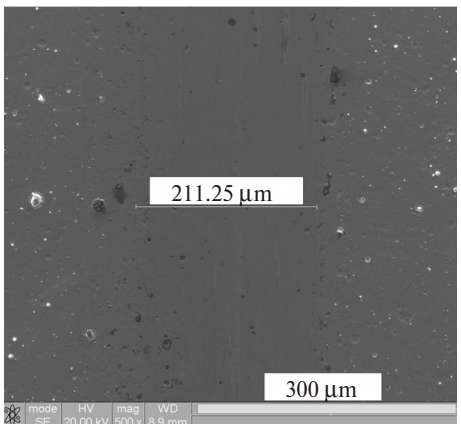

(c)

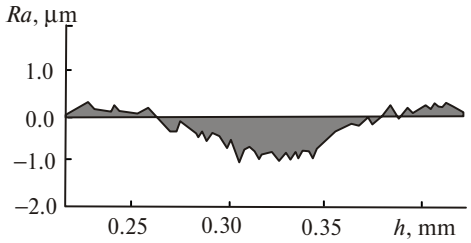

(d)

Fig. 5. Initial surface of the Mo_2N/CrN coating, deposited at $p_N = 3 \times 10^{-3}$ Torr (a), contact region of the counterbody (b), wear track on the coating (c) and its transverse profile (d).

As is seen from these images and Table 1, in testing the Mo_2N/CrN coatings deposited at $p_N = 3 \times 10^{-3}$ Torr there is an adhesion wear caused by the material transfer from one contact surface on the other and manifesting itself in the uniform wear of the coating with the profile wear track of a symmetric form and similar form of the counterbody (Figs. 5b–5d). According to [15], in this case the amount of the transferred material depends on the strength of the adhesion bond, which is defined by the electron structures of the Al_2O_3 counterbody and Mo_2N/CrN coating, their ability to form solid solutions or intermetallic compounds with one

another. If the Mo_2N/CrN coating was produced at the pressure $p_N = 7 \times 10^{-4}$ Torr, the mechanism of the abrasive wear takes place (see the profile of the wear track in Fig. 4d). This is caused by both the features of the coatings formations (the presence of large drops inside and on the surface of coatings) and interfacial disagreement of two different in type crystal lattices in nitride layers.

The destruction of coatings during the scratch-test in scratching with a diamond indenter may be divided into several stages. At the beginning a monotonic penetration of the indenter into a coating occurs and the coating exhibits an essential resistance to the indenter penetration, the friction coefficient, μ, nonmonotonically increases, the AE signal remains unchanged. Then as the load increases, the AE amplitude changes less intensively than the friction coefficient.

Figure 6a represents the averaged values of the friction coefficient and AE amplitude for a Mo_2N/CrN coating produced at $p_N = 7 \times 10^{-4}$ Torr and bias voltage $U_b = 70$ V. It is seen that on the medium region of the wear track at the friction coefficient close to 0.42 the AE caused by the structure imperfection and, particularly by a brittle fracture, maintains an intermittent form. A correlation with the parameters of the wear tracks in the region of loads, corresponding to the critical points L_{c1} and L_{c2} (see Figs. 6b and 6c) shows that the intermittent form of the dependence stems from the brittle fracture of the coating and its spalling.

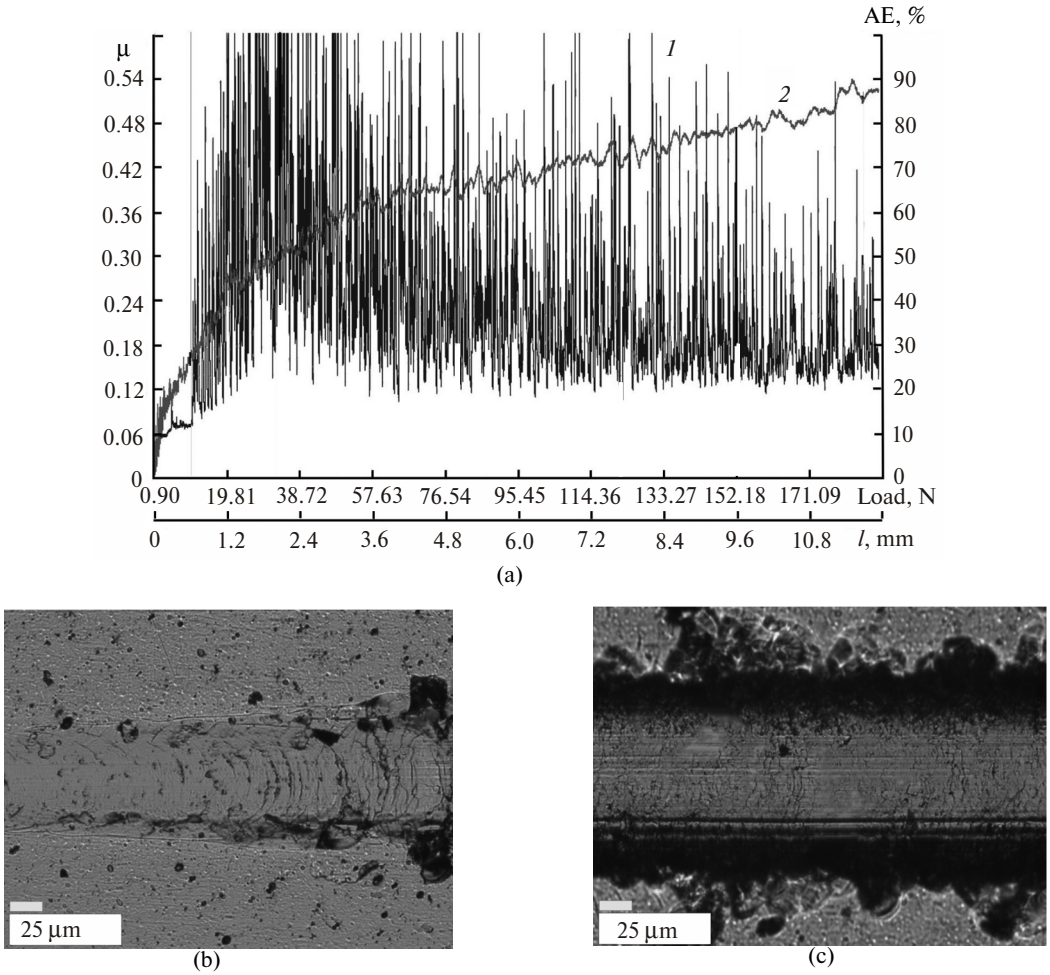

Fig. 6. Variation of averaged values of a friction coefficient (spectrum *2*) and AE amplitude (spectrum *1*) (a) depending on the load along the length of wear track; picture of the wear track in the region of loads, corresponding to the critical points L_{c1} (b) and L_{c2} (c), for Mo_2N/CrN coating produced at the pressure $p_N = 7 \times 10^{-4}$ Torr and negative bias voltage $U_b = 70$ V.

Unlike coatings produced at low pressure of the working atmosphere, over the whole range of the bias voltage values under study in the course of the coatings formation at $p_N = 3 \times 10^{-3}$ Torr a smooth shape of the AE curve is observed (Fig. 7).

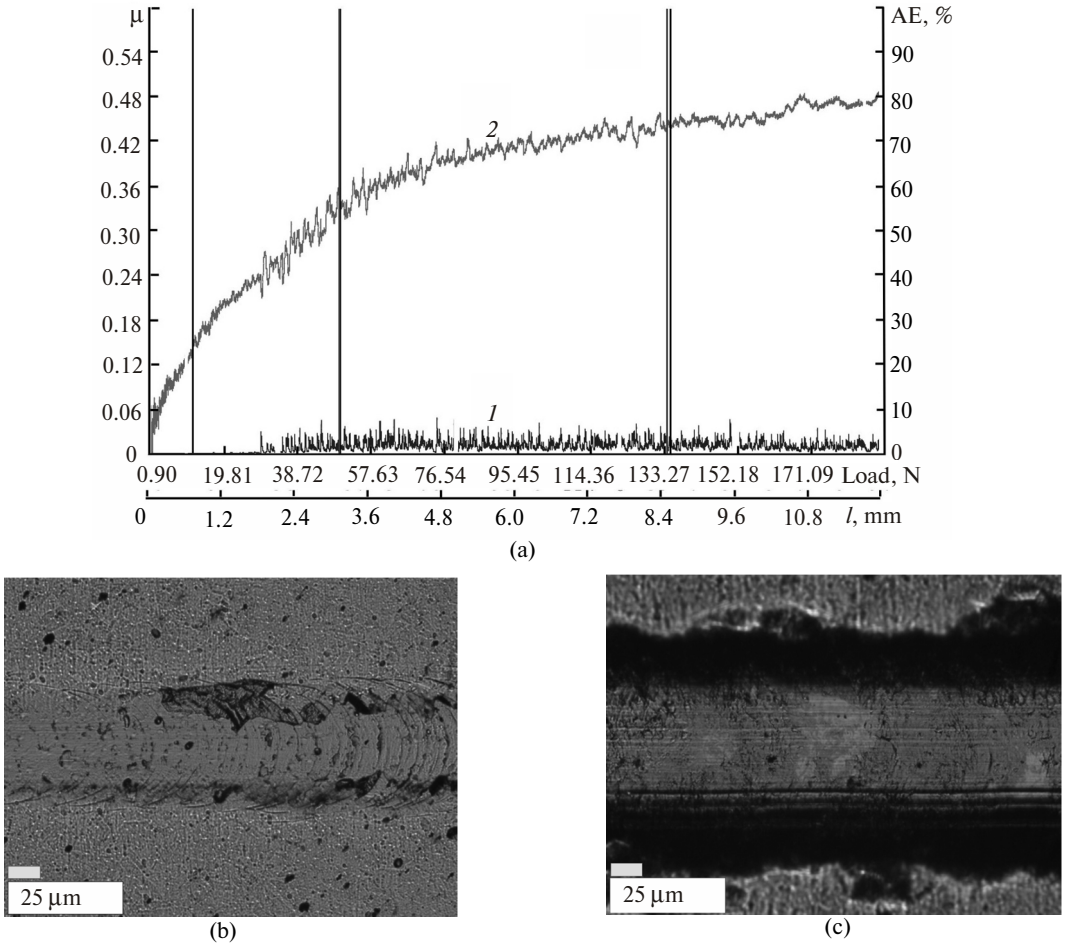

Fig. 7. Variation of averaged values of the friction coefficient (spectrum *2*) and AE amplitude (spectrum *1*) (a); picture of the wear track in the region of loads, corresponding to the critical points L_{c1} (b) and L_{c2} (c), for Mo_2N/CrN coating produced at pressure $p_N = 7 \times 10^{-4}$ Torr and negative bias voltage $U_b = 70$ V.

The analysis of the critical load of breaking coating under the indenter shows that at the high pressure of the coating formation (see Fig. 7) the critical load attains 135 N.

Cracking of coatings with a high initial defectiveness produced at $p_N = 7 \times 10^{-4}$ Torr occurs actively even at low loads, which is supported by the nature of the AE signals (see Fig. 6a) and micrographs that show gradually growing transverse cracking of the coating. In this case the critical load is lower by almost a factor of 2.5 and is 59 N.

Generalized critical loads for L_{c1}, L_{c2}, and L_{c3} points of coating, produced at different negative bias voltages and pressures are listed in Table 2.

Table 2. Critical loads L_c for coatings produced at different conditions of deposition

Conditions of deposition		Critical loads, N		
U_b, V	p_N, Torr	L_{c1}	L_{c2}	L_{c3}
20	3×10^{-3}	11	40	71
70	3×10^{-3}	12	50	145
70	7×10^{-4}	10	33	59
150	3×10^{-3}	8	53	159
150	7×10^{-4}	9	31	56
300	3×10^{-3}	13	46	137

With increasing modulus of the bias voltage, U_b, at which due to the atomic peening the material compaction takes place [2], the increase of the critical loads is observed. The comparative analysis of condensates obtained at high pressure indicates that in scratching coatings wear, but do not flake, i.e., they fracture by the cohesion mechanism, caused by the plastic deformation and formation of fatigue cracks in the coating material [16].

At low pressure ($p_N = 7 \times 10^{-4}$ Torr) because of the lower concentration of nitrogen atoms in the coating, in the chromium nitride layers the formation of a lower nitride, β-Cr_2N, with a hexagonal crystal lattice takes place. This decreases the cohesion interaction between layers in a multilayer coating. Correspondingly, the critical stresses that such a coating can withstand decrease and the fracture is of a brittle cracking nature.

4. CONCLUSIONS

As the working pressure of the nitrogen atmosphere has been decreased from 3×10^{-3} to 7×10^{-4} Torr, the Mo_2N/CrN coating depletes in nitrogen. At the phase and structure level this results in the transition of two similar cubic structures γ-Mo_2N with a wide region of homogeneity in layers of molybdenum and chromium nitrides to the formation of the lower in nitrogen β-Cr_2N phase with a hexagonal crystal lattice in the CrN layer.

Coatings hardness attains 38 GPa and decreases with decreasing pressure at the deposition and supply of negative bias voltage, which stimulates a selective secondary sputtering and depletion of the coating in light nitrogen atoms.

Coatings that have been produced at pressure 3×10^{-3} Torr, which are characterized by the formation of nitrogen isostructural (with a cubic lattice) layers, the wear occurs by the adhesion type with the comparable values of the coating and counterbody wear. The wear of coatings that are produced at $p_N = 7 \times 10^{-4}$ Torr and have nonisostructural types of crystal lattices (hexagonal and cubic) in nitrogen layers has signs of an abrasive brittle type and the coating wear far exceeds that of the counterbody.

The investigation of the adhesion and strength characteristics by the scratch–test shows that at the decrease of the nitrogen pressure the nature of coating fracture changes from the plastic abrasion to brittle fracture. A variation of the modulus of the bias voltage in the range from 20 to 300 V does not principally affect the type of the coating fracture.

The highest critical load of fracture (145–159 N) is characteristic of coatings that has been deposited at the $p_N = 3 \times 10^{-3}$ Torr and negative bias voltage $U_b = 70–150)$ V.

REFERENCES

1. Pogrebnjak, A.D., Shpak, A.P., Azarenkov, N.A. and Beresnev, V.M., Structure and properties of hard and superhard nanocomposite coatings, *Physics–Uspekhi*, 2009, vol. 179, no. 1, pp. 35–64.
2. Sobol' O. V., Control of the structure and stress state of thin films and coatings in the process of their preparation by ion–plasma methods, *Phys. Solid State*, 2011, vol. 53, no. 7, pp. 1464–1473.
3. Lukaszkowicz, K., Dobrzañski, L.A., Zarychta, A., and Cunha, L., Mechanical properties of multilayer coatings deposited by PVD techniques onto the brass substrate, *J. Achiev. Mater. Manuf. Eng.*, 2006, vol. 15, no. 1–2, pp. 47–52.
4. Sobol', O.V., Andreev, A.A., Grigoriev, S.N., et al., Effect of high-voltage pulses on the structure and properties of titanium nitride vacuum-arc coatings, *Metal Sci. Heat Treat.*, 2012, vol. 54, no. 3–4, pp. 195–203.
5. Samani, M.K., Ding, X.Z., Khosravian, N., et al., Thermal conductivity of titanium nitride/titanium aluminum nitride multilayer coatings deposited by lateral rotating cathode arc, *Thin Solid Films*, 2015, vol. 578, pp. 133–138.
6. Sobol', O.V., Andreev, A.A., Stolbovoi, V.A., and Fil'chikov, V.E., Structural-phase and stressed state of vacuum-arc-deposited nanostructural Mo–N coatings controlled by substrate bias during deposition, *Tech. Phys. Lett.*, 2012, vol. 38, no. 2, pp. 168–171.
7. Lackner, J.M., Waldhauser, W., Majo, L., and Kot, M., Tribology and micromechanics of Chromium Nitride Based Multilayer Coatings on Soft and Hard Substrates, *Coatings*, 2014, vol. 4, pp. 121–138.
8. Guglya, A.G. and Neklyudov, I.M., Coatings based on chromium nitride. Experience on the development and investigation, *Physics Metals–Uspekhi*, 2005, vol. 6, pp. 197–232.
9. Gilewicz,' A. and Warcholinski, B., Tribological properties of CrCN/CrN multilayer coatings, *Tribol. Int.*, 2014, vol. 80, pp. 34–40.
10. Ertas, M., Onel, A.C., Ekinci, G., et al., Arslan Investigation of VN/TiN Multilayer Coatings on AZ91D Mg Alloys, *Int. J. Chem., Nuclear, Mater. Metall. Eng.,* 2015, vol. 9, no. 1, pp. 53–57.

11. Xie, Z.H., Hoffman, M., Munroe, P., et al., Microstructural response of TiN monolithic and multilayer coatings during microscratch testing, *J. Mater. Res.*, 2007, vol. 22, no. 8, pp. 2312–2318.

12. Pogrebnjak, A.D., Pshik, A.V., Beresnev, V.M., and Zhollybekov, B.R., Protection of samples from friction and wear using titanium-based multicomponent nanocomposite coatings, *J. Friction and Wear*, 2014, vol. 35, no. 1, pp. 72–85.

13. Andreyev, A.A., Sablev, L.P., and Grigor'ev, S.N., *Vakuumno-dugovye pokrytiya* (Vacuum–arc coatings), Kharkov: NSC KhPhTI, 2010.

14. Ibatullin, I.D., *Kinetika ustalostnoi povrezhdaemosti i razrusheniya poverkhnostnykh sloev: monographiya* (Kinetics of fatigue damageability and fracture of surface layers: monograph), Samara, RF: Samara State Technical University, 2008.

15. Myshkin, P.K. and Petrokovets, M.I., *Trenie, smazka, iznos. Fizicheskie osnovy i technicheskie prilozheniya tribologii* (Friction, lubrication, wear. Physical fundamentals and technical applications of the tribology), Moscow: Fizmatlit, 2007.

16. Grigoriev, S.N., Sobol, O.V., Beresnev, V.M., et al., Tribological characteristics of (TiZrHfVNbTa)N coatings applied using the vacuum arc deposition method, *J. Friction Wear*, 2014, vol. 35, no. 5, pp. 359–364.

Translated by G. Kostenchuk